PERIÓDICO TCHÊ QUÍMICA
ARTIGO ORIGINAL

SYNTHESIS AND PHOTOPHYSICAL PROPERTIES OF NEW DIPHENYLACRYLONITRILE-BEARING ALDEHYDES

SÍNTESE E PROPRIEDADES FOTOFÍSICAS DE NOVOS ALDEÍDOS CONTENDO DIFENILACRILONITRILA

التخليق و الخصائص الفيزيائية الضوئية للألدهيدات الجديدة الحاملة لثنائي فينيل أكريلونيتريل

Rehab Katan Aflouk
University of Misan, College of Science, Department of Chemistry, Iraq.

Usama Ali Muhsen*
University of Misan, College of Science, Department of Chemistry, Iraq.

Ali Kareem A. Al-Lami
University of Misan, College of Science, Department of Chemistry, Iraq.

** Corresponding author*
e-mail: usama.muhsen@uomisan.edu.iq

Received 19 November 2023; received in revised form 08 February 2024; accepted 14 November 2024

RESUMO

Introdução: Através de uma simples condensação aldólica ciano e controlando a temperatura, dois aldeídos contendo difenilacrilinitrila foram sintetizados, e suas estruturas foram confirmadas por técnicas de infravermelho, ^{1}H, ^{13}C-RMN e massa. Suas propriedades fotofísicas também foram estudadas em diferentes solventes orgânicos polares e não polares (clorofórmio, THF e DMSO). Os máximos de absorção dos compostos variam entre (300-400 nm), enquanto os espectros de emissão variam entre (400-500 nm) com deslocamento de Stokes vermelho entre 68-86 nm. A adição de água em suas soluções de THF ligeiramente melhorou sua característica de emissão induzida por agregação (AIE). **Objetivos:** Síntese de unidades de acrilonitrila via condensação aldólica ciano, controle de temperatura e estudo da atividade AIE. **Métodos:** A síntese de unidades de acrilonitrila de difenil ocorreu em duas etapas: 1- Por meio da o-arilação, aldeídos lineares foram sintetizados, 2- Adicionando gradualmente cianeto de p-ansiyl aos aldeídos lineares em um balão redondo contendo metanol e KOH. **Resultados:** Unidades de acrilonitrila de difenil foram sintetizadas, e suas estruturas foram verificadas usando IR, ^{1}HNMR, ^{13}CNMR e técnicas de massa. Os resultados fotofísicos forneceram dados indicando que os compostos de aldeídos contendo difenilacrilinitrila possuem fluorescência com um comprimento de onda variando entre 400-500 nm e atividade AIE moderada. **Discussões:** As unidades de aldeídos contendo difenilacrilinitrila preparadas mostraram atividade AIE moderada no estado de agregação, onde a intensidade de fluorescência aumenta com o aumento da porcentagem de água na mistura THF/H_2O e atinge o pico em 80%. A razão reside no fato de que o grupo ciano forma acrilonitrila com estruturas torcidas, o que evita ACQ e aprimora as propriedades AIE. **Conclusões:** controlando a temperatura e através de uma condensação aldólica fácil, unidades de fenilacrilinitrila foram sintetizadas em bons rendimentos. Suas propriedades fotofísicas foram estudadas, e constatou-se que possuem atividade AIE moderada.

Palavras-chave: *Difenilacrilinitrila, rendimentos quânticos, emissão induzida por agregação (AIE), deslocamento de Stokes*.

ABSTRACT

Background: The cyano group is well-known for its strong electron-withdrawing properties, Effective in producing acrylonitrile when added to π-conjugated alkene structures. The twisted structures of acrylonitrile help avoid the ACQ phenomenon and induce AIE properties, making acrylonitrile units important in various applications**. Aims:** Synthesis of acrylonitrile units via cyano aldol condensation by temperature control and study of AIE activity. **Methods:** The synthesis of diphenyl acrylonitrile units took place in two steps: 1- By o-arylation, linear aldehydes were synthesized, 2- Gradually adding *p*-ansiyl cyanide to the linear aldehydes in a round flask containing methanol and KOH. **Results:** Diphenyl acrylonitrile units were synthesized, and their structures were identified using IR, ^{1}HNMR, ^{13}CNMR, and mass techniques. The photophysical results indicated

DOI: 10.52571/PTQ.v21.n48.2024_13_Ali_pgs_152_171.pdf

that diphenylacrylonitrile-bearing aldehyde compounds have fluorescence with a wavelength ranging between 400-500 nm and moderate AIE activity**. Discussion:** The prepared diphenylacrylonitrile-bearing aldehydes units showed moderate AIE activity in the aggregation state, where the fluorescence intensity increases with increasing water percentage in the THF/H_2O mixture and reaches its peak at 80%. The reason lies in the fact that the cyano group forms acrylonitrile with twisted structures, which avoids ACQ and enhances the AIE properties. **Conclusions:** by controlling the temperature and through a facile aldol condensation, phenylacrylonitrile units were synthesized in good yields. Their photophysical properties were studied, and they were found to have moderate AIE activity.

Keywords: *Diphenylacrylonitrite, quantum yields, aggregation-induced emission (AIE), Stokes shift.*

الملخص

الخلفية: تعتبر مجموعة السيانو من افضل المجاميع الساحبة للالكترون ، وهي فعالة بشكل خاص في إنتاج الأكريلونيتريل عندما تُضاف إلى هياكل الألكين المتعاقبة. تساهم التراكيب الملتوية للأكريلونيتريل في تجنب ظاهرة تخميد التجمع (ACQ) وتحفيز خصائص التجمع الناجم عن الانبعاث الخاص بالفلورة الجزيئية (AIE)، مما يجعل وحدات الأكريلونيتريل مهمة في مجموعة متنوعة من التطبيقات. **الأهداف**: تصنيع وحدات الأكريلونيتريل عن طريق تكثيف السيانو ألدول، والتحكم في درجة الحرارة، ودراسة فعالية التجمع الناتج عن الانبعاث. **طرائق العمل:** تم تصنيع وحدات ثنائي فينيل أكريلونيتريل على خطوتين: 1- بواسطة الأريلة تم تصنيع الألدهيدات الخطية، 2- إضافة *p*-ansiyl cyanide تدريجياً إلى الألدهيدات الخطية في دورق دائري يحتوي على الميثانول وهيدروكسيد البوتاسيوم. **النتائج:** تم تصنيع وحدات ثنائي فينيل أكريلونتريل، وتم التحقق من بنيتها بأستخدام تقنيات الأشعة تحت الحمراء، ^{1}H, ^{13}C-NMR وطيف الكتلة. أعطت النتائج الفيزيائية الضوئية بيانات تشير إلى أن مركبات الألدهيدات الحاملة لثنائي فينيل أكريلونيتريل تمتلك فلورة بطول موجي يتراوح بين 400-500 نانومتر وفعالية معتدلة من التجمع الناجم عن الانبعاث. **المناقشة:** أظهرت وحدات الألدهيدات الحاملة لثنائي فينيل أكريلونيتريل نشاط معتدل من التجمع الناجم عن الانبعاث، حيث تزداد شدة التألق مع زيادة نسبة الماء في خليط THF/H_2O وتصل إلى ذروتها عند 80%. السبب يكمن في حقيقة أن مجموعة السيانو تجعل الأكريلونيتريل بهياكل ملتوية، مما يتجنب تخميد التجمع ويعزز خصائص التجمع الناجم عن الانبعاث. **الاستنتاجات:** من خلال التحكم في درجة الحرارة ومن خلال تكثيف الألدول البسيط، تم تصنيع وحدات الفينيل أكريلونيتريل في عوائد جيدة. تمت دراسة خصائصها الفيزيائية الضوئية، ووجد أن نشاطها معتدل من التجمع الناجم عن الانبعاث الخاص بالفورة الجزيئية.

الكلمات المفتاحية : ثنائي فينيل أكريلينيتريل، عائد الكم، ظاهرة التجمع الناجم عن الانبعاث الخاص بالفورة الجزيئية **(AIE)** ، تحول ستوكس

1. INTRODUCTION:

The cyano group is considered one of the best electron-withdrawing groups, which, when added to the π-conjugated structures of alkenes, results in acrylonitriles (scheme 1) that have unique alterations in their conformation, stability, packing mode, processability, and solubility (C. Wang *et al*., 2017; Xing *et al*., 2016; Zhao et *al*., 2018).

Further, acrylonitriles are an example of a typical structural pattern commonly found in agrochemicals, pharmaceuticals, herbicides, and natural products (Fleming et al., 1999; Fleming et al., 2010). More importantly, a donor can be introduced to the acrylonitrile skeleton to create fluorescent materials with acceptor and donor-conjugated structures and nonlinear optical characteristics, which are excellent for two-photon excited imaging in live samples due to high spatial resolution, deep tissue penetration, and minimal background fluorescence (Guo *et al*., 2014; C. Wang et al., 2017). Recently, great efforts have been made to synthesize acrylonitriles with diverse functions and substitutions.(Barrado *et al*., 2017; Chaitanya *et al*., 2015; Paquin *et al*., 2015; X. Wang *et al*., 2018). Allyl azides were synthesized by reacting allyl halides or esters with NAN_3 or $TMSN_3$ catalyzed by $Pd(PPh_3)_4$ and then converting them to alkenyl nitriles (or acrylonitriles) using DDQ as the oxidant (Scheme 1) (T. Wang *et al*., 2014). On the other hand, for the purpose of developing various acrylonitriles, the direct cyanation route of alkenes has also been adopted (Chaitanya *et al*., 2015; Gao *et al*., 2018; Su *et al*., 2015; X. Wang *et al*., 2018). Engle *et al*. reported novel oxidative cyanation of terminal and internal alkenes utilizing a homogeneous copper catalyst to obtain acrylonitrile (Gao *et al*., 2018). Accordingly, many acrylonitriles have been synthesized. Still, these methods require hazardous and toxic agents, harsh reaction conditions, low atomic economy, and expensive transition metal complexes. Direct functionalities of acrylonitriles are still challenging, and this area needs further improvement. Via a transition metal-free, non-toxic, nonhazardous, and atom-economic nucleophilic reaction, research groups discovered that aldehydes or ketones and propane nitriles were reactants for direct production of acrylonitriles using conventional bases such as NaOH, t-BuOK. (Lee *et al*., 2013; Shi *et al*., 2016; Wei *et al*., 2018; Zhu *et al*., 2012). As a result, this kind of nucleophilic reaction may have enormous promise for the facile and direct synthesis of versatile acrylonitriles with various functionalities.

The aggregation-induced emission (AIE) effect was reported by Tang's group (Hong *et al*.,

2009, 2011; Luo *et al*., 2001; M. Wang *et al*., 2010). AIE is a particular photophysical phenomenon in which some luminous gives off weak or no fluorescence in solution, but the emission increases greatly in the aggregated and solid state (Chen *et al*., 2019; He *et al*., 2019; Hu *et al*., 2018; Y. J. Li *et al*., 2019; Ni *et al*., 2018). Previous studies have shown that cyano groups make the acrylonitrile with twisted structures, which leads to avoiding aggregation-caused quenching (ACQ) and AIE properties in the aggregate state in aqueous environment (B. K. An *et al*., 2002; Lim *et al*., 2004). Many multicolor brightly emissive AIE luminogens (AIEgens) have been synthesized based on acrylonitriles and applied in various fields such as one- and two-photon bioimaging and fluorescence sensing (K. Y. Kim *et al*., 2018; Mandal *et al*., 2015; C. Y. Y. Yu *et al*., 2017). Because of the minimal background autofluorescence, deep tissue penetration, and reduced photodamage, acrylonitriles with bright red emission are particularly preferred in bioimaging (Haque *et al*., 2017; J. Bin Li *et al*., 2019; Yuan *et al*., 2013). Unfortunately, acrylonitrile-based AIEgens with highly red-emissive are still rare (B. An *et al*., 2009; M. Kim *et al*., 2015; Lu *et al*., 2016; Paramasivam *et al*., 2016; Zhang *et al*., 2014). In addition, their synthesis involves multi-step reaction methods and time-consuming isolation or purification due to their complicated structures (Niu *et al*., 2019).

This work aims to synthesize different acrylonitriles bearing aldehydes via metal-free, non-toxic, and atom-economic transformation through cyano aldol condensation. The photophysical properties of the prepared acrylonitriles were also evaluated.

2. MATERIALS AND METHODS:

Provide sufficient details to permit repetition of the experimental work. A technical description of the methods should be given when they are new.

2.1. Materials

The following materials were used in this study: p-hydroxybenzaldehyde, p-anisyl cyanide, 1,3-dibromopropane, 1,4-dibromobutane, anhydrous sodium carbonate, potassium hydroxide, dichloromethane, chloroform, tetrahydrofuran, dimethyl sulfoxide, N,N-dimethylformamide (laboratory reagent grade), petroleum ether, ethanol, methanol, and silica gel (100–200 mesh).

2.2. Methods

2.2.1 Method of Synthesis of 4,4'-[alkane-1,2-diylbis(oxy)]dibenzaldehyde (R1 and R2)

At room temperature, 4-hydroxybenzaldehyde (81.9 mmol), dibromoalkane [$(CH_2)_n$ n = 3, 4] (40.9 mmol), and Na_2CO_3 (163.8 mmol) were added to a two-necked round-bottomed flask containing DMF (50 ml). The mixture was stirred and heated to reflux (140 °C for 6 h). TLC monitored the reaction until the reaction was completed. After completion of the reaction, the mixture was allowed to cool to room temperature and quenched with distilled water, filtered and washed with water, and dried to obtain a crude product. The crude products were recrystallized from ethanol to give an off-white solid 4,4'-[alkane-1,2-diylbis(oxy)] dibenzaldehyde in excellent purity. (Devaraju *et al*., 2013)

2.2.2 Method of Synthesis diphenylacrylonitrile-bearing aldehydes (R3 and R4)

A p-anisyl cyanide (0.774 mmol in 5ml of methanol) was added gradually (dropwise) to a two-necked round flask containing (0.704 mmol) of 4,4'-[alkane-1,2-diylbis(oxy)] dibenzaldehyde (R1 and R2), KOH (1.76 mmol), (20 ml) methanol at temperature (50 ^oC for 30 min). After completing the addition, the mixture was stirred and heated to reflux (for 24 hours). TLC monitored the reaction until the reaction was completed after completion of the reaction. The mixture was filtered, the filtrate was taken and dried by a rotary evaporator, and the product was purified via silica gel column chromatography using (DCM: Petroleum ether; 3:2) as eluent to give the product as a solid in excellent purity. (Q. Yu *et al*., 2020).

2.2.3 Method for measuring the photophysical properties of diphenylacrylonitrile-bearing aldehydes(R3 and R4)

Solutions with a concentration of (1×10^{-5} M) were prepared, and the absorbance was measured in a number of polar and nonpolar solvents (DMSO, THF, chloroform), and fluorescence was measured at the same concentration. UV-visible spectra were recorded on the Shimadzu UV-spectrophotometer (UV-1800), and Fluorescence spectra were obtained on the Shimadzu spectrofluorophotometer (RF-5301pc). UV-vis and fluorescence spectra were

plotted using the spectrograph program (software for optical spectroscopy, version 1.2.16.1).

2.2.4 Method of studying AIE behavior for diphenylacrylonitrile-bearing aldehydes (R3 and R4)

The effect of AIE on the THF/H_2O was studied. This was done by preparing a solution of R3 and R4 in proportions from 0 to 80% and measuring the fluorescence at 350 nm (whereas λ_{ex} of diphenylacrylonitrile = 350nm).

2.2.5 Method for calculation of the quantum yields

The fluorescence quantum yields of the compounds R3 and R4 in chloroform, THF, and DMSO were calculated using the relative Method (comparison method). The quantum yields of a sample are calculated by comparing the fluorescence intensity with another sample of known quantum yields as a reference. This requires knowing the absorbance of both the sample and the reference (Tryptophan was used as a reference in the fluorescence spectrum), considering the refractive index of the solvents used (Brouwer, 2011; Suzuki *et al.*, 2009).

3. RESULTS AND DISCUSSION:

3.1. Results

3.1.1. Spectroscopic characterization of linear aldehydes (R1 and R2)

3.1.1.1 4,4'-[alkane-1,2-diylbis(oxy)]dibenzal-dehyde (R1 and R2) 4,4'-(propane-1,3-diylbis(oxy))diben zaldehyde (R1):

White crystals. Yiled 51% , m.p.124-125 ˚C; IR (KBr): 2947 (CH_2), 3070 (CH-Ar), 1693 (C=O), 1600 (C=C), 1111 (C-O) cm^{-1},^{1}H-NMR (400 MHz, DMSO-d_6): ppm δ 9.86 (s, 2H, C*H*O), 7.86 (s, 4H, Ar-*H*), 7.15 (s, 4H, Ar-*H*), 4.26 (s, 4H, OCH_2), 2.24 (s, 2H, CH_2), ^{13}C-NMR (100 MHz, DMSO-d_6): ppm δ 191.4 (*C*=O ×2), 163.5 (Ar-*C* ×2), 131.9 (Ar-*C*H ×4), 129.7 (Ar-*C* ×2), 115.0 (Ar-*C*H ×4), 64.8 (O*C*H_2 ×2), 28.3 (*C*H_2).

3.1.1.2. 4,4'-(butane-1,4-diylbis(oxy))dibenz- aldehyde (R2):

Golden crystals. Yield 52%, m.p. 98-100 ˚C; IR (KBr): 2951 (CH_2), 3059 (CH-Ar), 1685 (C=O), 1604 (C=C), 1111 (C-O) cm^{-1} ,^{1}H-NMR (400 MHz, DMSO-d_6): ppm δ 9.86 (s, 2H, C*H*O), 7.85 (s, 4H, Ar-*H*), 7.11 (s, 4H, Ar-*H*), 4.15 (s, 4H, OCH_2), 1.90 (s, 4H, CH_2), ^{13}C-NMR (100 MHz, DMSO-d_6): ppm δ 191.3 (*C*=O ×2), 163.6 (Ar-*C* ×2), 131.9 (Ar-*C*H ×4), 129.6 (Ar-*C* ×2), 114.9 (Ar-*C*H ×4), 67.7 (O*C*H_2 ×2), 25.2 (*C*H_2 ×2).

3.1.3. Spectroscopic characterization of diphenylacrylonitrile-bearing aldehydes (R3 and R4)

3.1.3.1. (Z)-3-(4-(3-(4-formylphenoxy) propo-xyphenyl)-2-(4methoxyphenyl)acry-lonitrile (R3):

Light green crystals. Yield 47% m.p. 103-105 ˚C; IR (KBr): 2943-2885 (aliph.C-H), 3032 (Ar. C-H), 1685 (C=O), 1600 (C=C), 1118 (C-O) , 1361 (C-N) cm^{-1} ; ^{1}H-NMR (400 MHz, DMSO-d_6): ppm δ 9.86 (s, 1H, C*H*O), 7.85-7.91 (m, 4H, Ar-*H*), 7.81 (s, 1H, C=C*H*), 7.65 (d, 2H, J= 8.7 Hz, Ar-*H*), 7.15 (d, 2H, J= 8.6 Hz, Ar-*H*), 7.11 (d, 2H, J= 8.6 Hz, Ar-*H*), 7.05 (d, 2H, J= 8.7 Hz, Ar-*H*), 4.26 (t, 2H, J= 6.0 Hz, OCH_2), 4.22 (t, 2H, J= 6.0 Hz, OCH_2), 3.80 (s, 3H, CH_3), 2.24 (quin, 2H, J= 6.0 Hz, CH_2); ^{13}C-NMR (100 MHz, DMSO-d_6): ppm δ 191.3 (*C*=O), 163.5 (Ar-*C*), 160.0 (Ar-*C*), 159.8 (Ar-*C*), 140.3 (*C*H=C), 131.9 (Ar-*C*H ×2), 130.9 (Ar-*C*H ×2), 129.7 (Ar-*C*), 126.9 (Ar-*C*H ×2), 126.6 (Ar-*C*), 126.5 (Ar-*C*), 118.5 (*C*N), 115.0 (Ar-*C*H ×2), 114.9 (Ar-*C*H ×2), 114.6 (Ar-*C*H ×2), 106.9 (*C*), 64.8 (O*C*H_2), 64.4 (O*C*H_2), 55.4 (*C*H_3), 28.4 (*C*H_2); HRMS (ESI+) m/z: (M+Na^+) calcd $C_{26}H_{23}NNaO_4^+$ 436.1525, found 436.1524.

3.1.3.2. (Z)-3-(4-(4-(4-formylphenoxy)butoxy) phenyl)-2-(4-methoxyphenyl)acrylonitrile (R4):

White crystals. Yield 45% , m.p. 123-125 ˚C; IR (KBr): 2943 (aliph.C-H), 3028 (Ar. C-H), 1689 (C=O), 1600 (C=C), 1111 (C-O) cm^{-1} ,1392 (C-N); ^{1}H-NMR (400 MHz, DMSO-d_6): ppm δ 9.86 (s, 1H, C*H*O), 7.85-7.91 (m, 4H, Ar-*H*), 7.82 (s, 1H, C=C*H*), 7.65 (d, 2H, J= 8.7 Hz, Ar-*H*), 7.04-7.14 (m, 6H, Ar-*H*), 4.12-4.16 (m, 4H, OCH_2 ×2), 3.80 (s, 3H, CH_3), 1.91 (m, 4H, CH_2 ×2); ^{13}C-NMR (100 MHz, DMSO-d_6): ppm δ 191.3 (*C*=O), 163.6 (Ar-*C*), 160.2 (Ar-*C*), 159.8 (Ar-*C*), 140.4 (*C*H=C), 131.8 (Ar-*C*H ×2), 130.8 (Ar-*C*H ×2), 129.6 (Ar-*C*), 126.9 (Ar-*C*H ×2), 126.5 (Ar-*C*), 126.4 (Ar-*C*), 118.6 (*C*N), 114.9 (Ar-*C*H ×2), 114.8 (Ar-*C*H ×2), 114.6 (Ar-*C*H ×2), 106.8 (*C*=CH), 67.7 (O*C*H_2), 67.4 (O*C*H_2), 55.4 (*C*H_3), 25.2 (*C*H_2 ×2); HRMS (ESI+) m/z: (M+H^+) calcd $C_{27}H_{25}NO_4^+$ 428.1862, found 428.1857.

3.2. Discussion

3.2.1 Synthesis and characterization

The diphenylacrylonitrile-bearing aldehydes R3 and R4 were synthesized with good yield in two steps (Scheme 2); (i) by o-arylation, linear dialdehydes were synthesized, using the 4-hydroxy benzaldehyde and dibromoalkane [$(CH_2)_n$ n = 3, 4] in the presence of anhydrous sodium carbonate in DMF. (ii) The linear dialdehyde R1 and R2 reacted with *p*-anisyl cyanide using the facile nucleophilic reaction in the presence of KOH in MeOH. IR, ^{1}H-NMR, ^{13}C-NMR, and mass spectra characterized the synthesized compounds.

3.2.1.1. 4,4'-[alkane-1,2-diylbis(oxy)]dib-enzaldehyde (R1 and R2)

The IR data of compounds R1 and R2 (Figure 1 and Figure 4), respectively, showed the bond (C=O) of aldehyde group stretching vibration appears in (1685-1693) cm^{-1}, and the 1H-NMR spectrum further confirmed this in (Figure 2 and Figure 5), respectively. ^{1}HNMR spectrum of the compounds showed one distinctive singlet at δ (9.86) ppm, confirming the presence of aldehydes protons, as well as the singlet at δ (7.11-7.86) ppm and δ (4.11-4.26) ppm, confirming the presence of aromatic and aliphatic protons, respectively. ^{13}CNMR spectrum of the compounds showed the appearance of a signal for C=O in aldehyde group at δ (191.3-191.4), while the signal of (OCH_2) carbon appears at δ (64.8-67.7) ppm and existence of a peak at δ (25.2-28.3) ppm belong to the presence of (CH_2) group, as shown in (Figure 3 and Figure 6).

3.2.1.2. Diphenylacrylonitrile-bearing aldehydes (R3 and R4)

The IR spectrum of R3 and R4 compounds showed absorption bands in regions (2943-2873) cm-1 and (3028-3032) cm^{-1}, which belong to aliphatic and aromatic C-H bonds. The bond (C=O) of aldehyde group stretching vibration appears in (1685-1689) cm^{-1} (Figure 7 and Figure 11). ^{1}HNMR spectrum of these compounds showed singlet at δ (9.86) ppm confirming the presence of aldehyde proton, aromatic protons peaks appear at δ (7.04-7.91) ppm, vinyl proton appears at δ (7.81-7.82) ppm, and protons of (OCH_2) exhibit at δ (4.12-4.4.26) ppm, while signal of (OCH_3) protons appears at δ (3.80) ppm as a singlet, protons of (CH_2) appears at δ (1.91) ppm (Figure 8 and Figure 12). In the ^{13}CNMR spectrum, signals at δ (191.3) ppm denote the presence of C=O in the aldehyde group, while the signals of aromatic carbons appear at δ (114.6-163.6) ppm. A signal of vinylic CH appears at δ (140.3-140.4) ppm, while the signal of vinylic C appears at δ (106-107) ppm. A signal of OCH_2 carbon appears at δ (67.4 -67.7) ppm, and a signal at δ (55.4) ppm belongs to the (CH_3) group, and the existence of a peak at δ (25.2-28.4) ppm belongs to the presence of CH_2 group (Figure 9 and Figure 13). The mass spectra of R3 and R4, shown in (Figure 10 and Figure 14) respectively, are identical with their calculated mass.

3.2.2 Photophysical properties for diphenylacrylonitrile-bearing aldehydes (R3, R4)

UV-vis absorption and emission spectra were measured in several different organic solvents to obtain an in-depth understanding of the photophysical properties of R3 and R4 (Figure 15, Figure 16, Figure 17, and Figure 18), the absorption spectra of the compounds show absorption peaks belonging to $\pi \rightarrow \pi^*$ (300-400 nm) for diphenylacrylonitrile group. It was observed that the two compounds R3 and R4 emit good fluorescence (400-500nm) in all use organic solvents due to the good solubility in these solvents. The effect of solvent polarity on the fluorescence spectra was studied, and it was noted that with increasing solvent polarity, the fluorescence spectra showed a red shift and a corresponding decrease in the fluorescence intensity. For compound R3, the maximum absorption limit in the absorption spectrum (λ_{abs}) ranged between 345-350 nm, while the maximum emission limit in the fluorescence spectrum (λ_{fl}) ranged between 417-434 nm, with a chemical red shift appearing as 72- 86 nm (Table 1). As for compound R4**,** the maximum absorption limit in the absorption spectrum (λ_{abs}) ranged between 342-350 nm, while the maximum emission limit in the fluorescence spectrum (λ_{fl}) ranged between 416-432 nm, with a chemical red shift appearing as 74-82 nm (Table 1).

To further explore the photophysical properties, mixtures of THF and water with different water fractions were used to investigate the aggregation-induced emission (AIE) behaviors. The fluorescence intensity of compounds R3 and R4 were investigated at λ_{ex}= 350 nm (Figure 19 and Figure 20). It is noted that when the water fraction increases, the fluorescence intensity of these compounds

increases gradually and attains a maximum of 80% because the cyano groups form acrylonitrile with twisted structures, avoiding aggregation-induced quenching (ACQ) and enhancing the AIE properties in the aggregate state in the aqueous environment. This result indicates that the compounds R3 and R4 have moderate AIE features.

4. CONCLUSIONS:

In conclusion, by controlling the temperature and through a facile aldol condensation, phenylacrylonitrile units were synthesized in good yields 47%, and their structures were confirmed by infrared, ^{1}H, ^{13}C-NMR, and mass techniques. Their photophysical properties were studied in several polar and nonpolar solvents (DMSO, THF, and chloroform). The effect of solvent polarity on the fluorescence spectra was studied, and it was noted that with increasing solvent polarity, the fluorescence spectra showed a red shift and a corresponding decrease in the fluorescence intensity. The effect of AIE was also studied for both compounds (Z)-3-(4-(3-(4-formylphenoxy)propoxy)phenyl)-2-(4methoxyphenyl)acrylonitrile (**R3**) and (Z)-3-(4-(4-(4-formylphenoxy)butoxy)phenyl)-2-(4-methoxyphenyl)acrylonitrile (**R4**) it was found that compounds R3 and R4 had moderate AIE activity.

5. DECLARATIONS

5.1. Study Limitations

The study is limited to the sample size and experimental conditions.

5.2. Acknowledgements

The authors want to thank the Chemistry Department for their assistance in completing this study.

5.3. Funding source

The authors funded this research.

5.4. Competing Interests

The authors declare no competing financial interest.

6. REFERENCES:

1. An, B., Gihm, S. H., Chung, J. W., Park, C. R., Kwon, S., & Park, S. Y. (2009). Color-Tuned Highly Fluorescent Organic Nanowires/Nanofabrics: Easy Massive Fabrication and Molecular Structural Origin. *Journal of the American Chemical Society*, *131*(11), 3950–3957. doi: 10.1021/ja806162h
2. An, B. K., Kwon, S. K., Jung, S. D., & Park, S. Y. (2002). Enhanced emission and its switching in fluorescent organic nanoparticles. *Journal of the American Chemical Society*, *124*(48), 14410–14415. doi: 10.1021/ja0269082
3. Barrado, A. G., Zieliński, A., Goddard, R., & Alcarazo, M. (2017). Regio- and Stereoselective Chlorocyanation of Alkynes. *Angewandte Chemie*, *129*(43), 13586–13590. doi: 10.1002/ange.201705851
4. Brouwer, A. M. (2011). Standards for photoluminescence quantum yield measurements in solution (IUPAC technical report). *Pure and Applied Chemistry*, *83*(12), 2213–2228. doi: 10.1351/PAC-REP-10-09-31
5. Chaitanya, M., & Anbarasan, P. (2015). Rhodium-Catalyzed Cyanation of C(sp 2)–H Bond of Alkenes. *Organic Letters*, *17*(15), 3766–3769. doi: 10.1021/acs.orglett.5b01746
6. Chen, Y., Lam, J. W. Y., Kwok, R. T. K., Liu, B., & Tang, B. Z. (2019). Aggregation-induced emission: Fundamental understanding and future developments. *Materials Horizons*, *6*(3), 428–433. doi: 10.1039/c8mh01331d
7. Devaraju, S., Prabunathan, P., Selvi, M.,

& Alagar, M. (2013). Low dielectric and low surface free energy flexible linear aliphatic alkoxy core bridged bisphenol cyanate ester based POSS nanocomposites. *Frontiers in Chemistry*, *1*(October), 1–10. doi: 10.3389/fchem.2013.00019
8. Fleming, F. F., & Fleming, F. F. (1999). Nitrile-containing natural products. *Natural Product Reports*, *16*(5), 597–606. doi: 10.1039/a804370a
9. Fleming, F. F., Yao, L., Ravikumar, P. C., Funk, L., & Shook, B. C. (2010). Nitrile-containing pharmaceuticals: Efficacious roles of the nitrile pharmacophore. *Journal of Medicinal Chemistry*, *53*(22), 7902–7917. doi: 10.1021/jm100762r
10. Gao, D.-W., Vinogradova, E. V, Nimmagadda, S. K., Medina, J. M., Xiao, Y., Suciu, R. M., Cravatt, B. F., & Engle, K. M. (2018). Direct Access to Versatile Electrophiles via Catalytic Oxidative Cyanation of Alkenes. *Journal of the American Chemical Society*, *140*(26), 8069–8073. doi: 10.1021/jacs.8b03704
11. Guo, L., & Wong, M. S. (2014). Multiphoton Excited Fluorescent Materials for Frequency Upconversion Emission and Fluorescent Probes. *Advanced Materials*, *26*(31), 5400–5428. doi: 10.1002/adma.201400084
12. Haque, A., Faizi, M. S. H., Rather, J. A., & Khan, M. S. (2017). Next generation NIR fluorophores for tumor imaging and fluorescence-guided surgery: A review. *Bioorganic and Medicinal Chemistry*, *25*(7), 2017–2034. doi: 10.1016/j.bmc.2017.02.061
13. He, Y., Li, Y., Su, H., Si, Y., Liu, Y., Peng, Q., He, J., Hou, H., & Li, K. (2019). An o-phthalimide-based multistimuli-responsive aggregation-induced emission (AIE) system. *Materials Chemistry Frontiers*, *3*(1), 50–56. doi: 10.1039/c8qm00454d
14. Hong, Y., Lam, J. W. Y., & Tang, B. Z. (2009). Aggregation-induced emission: Phenomenon, mechanism and applications. *Chemical Communications*, *29*, 4332–4353. doi: 10.1039/b904665h
15. Hong, Y., Lam, J. W. Y., & Tang, B. Z. (2011). Aggregation-induced emission. *Chemical Society Reviews*, *40*(11), 5361–5388. doi: 10.1039/c1cs15113d
16. Hu, F., Xu, S., & Liu, B. (2018). Photosensitizers with Aggregation-Induced Emission: Materials and Biomedical Applications. *Advanced Materials*, *30*(45), 1–29. doi: 10.1002/adma.201801350
17. Kim, K. Y., Jin, H., Park, J., Jung, S. H., Lee, J. H., Park, H., Kim, S. K., Bae, J., & Jung, J. H. (2018). Mitochondria-targeting self-assembled nanoparticles derived from triphenylphosphonium-conjugated cyanostilbene enable site-specific imaging and anticancer drug delivery. *Nano Research*, *11*(2), 1082–1098. doi: 10.1007/s12274-017-1728-7
18. Kim, M., Whang, D. R., Gierschner, J., & Park, S. Y. (2015). A distyrylbenzene based highly efficient deep red/near-infrared emitting organic solid. *Journal of Materials Chemistry C*, *3*(2), 231–234. doi: 10.1039/C4TC01763C
19. Lee, S., Chen, C. H., & Flood, A. H. (2013). A pentagonal cyanostar macrocycle with cyanostilbene CH donors binds anions and forms dialkylphosphate [3]rotaxanes. *Nature Chemistry*, *5*(8), 704–710. doi: 10.1038/nchem.1668
20. Li, J. Bin, Liu, H. W., Fu, T., Wang, R., Zhang, X. B., & Tan, W. (2019). Recent Progress in Small-Molecule Near-IR Probes for Bioimaging. *Trends in Chemistry*, *1*(2), 224–234. doi: 10.1016/j.trechm.2019.03.002
21. Li, Y. J., Zhang, H. T., Chen, X. Y., Gao, P. F., & Hu, C. H. (2019). A multifunctional AIEgen with high cell-penetrating ability for intracellular fluorescence assays, imaging and drug delivery. *Materials Chemistry Frontiers*, *3*(6), 1151–1158. doi: 10.1039/c9qm00089e
22. Lim, S. J., An, B. K., Sang, D. J., Chung, M. A., & Soo, Y. P. (2004). Photoswitchable organic nanoparticles and a polymer film employing multifunctional molecules with enhanced fluorescence emission and bistable photochromism. *Angewandte Chemie - International Edition*, *43*(46), 6346–6350. doi: 10.1002/anie.200461172
23. Lu, H., Zheng, Y., Zhao, X., Wang, L., Ma, S., Han, X., Xu, B., Tian, W., & Gao, H. (2016). Highly Efficient Far Red/Near-Infrared Solid Fluorophores: Aggregation-Induced Emission, Intramolecular Charge Transfer, Twisted Molecular Conformation, and Bioimaging Applications. *Angewandte Chemie - International Edition*, *55*(1), 155–159. doi: 10.1002/anie.201507031
24. Luo, J., Xie, Z., Xie, Z., Lam, J. W. Y.,

Cheng, L., Chen, H., Qiu, C., Kwok, H. S., Zhan, X., Liu, Y., Zhu, D., & Tang, B. Z. (2001). Aggregation-induced emission of 1-methyl-1,2,3,4,5-pentaphenylsilole. *Chemical Communications*, *18*, 1740–1741. doi: 10.1039/b105159h

25. Mandal, A. K., Sreejith, S., He, T., Maji, S. K., Wang, X.-J., Ong, S. L., Joseph, J., Sun, H., & Zhao, Y. (2015). Three-Photon-Excited Luminescence from Unsymmetrical Cyanostilbene Aggregates: Morphology Tuning and Targeted Bioimaging. *ACS Nano*, *9*(5), 4796–4805. doi: 10.1021/nn507072r
26. Ni, J. S., Zhang, P., Jiang, T., Chen, Y., Su, H., Wang, D., Yu, Z. Q., Kwok, R. T. K., Zhao, Z., Lam, J. W. Y., & Tang, B. Z. (2018). Red/NIR-Emissive Benzo[d]imidazole-Cored AIEgens: Facile Molecular Design for Wavelength Extending and In Vivo Tumor Metabolic Imaging. *Advanced Materials*, *30*(50), 1–9. doi: 10.1002/adma.201805220
27. Niu, G., Zheng, X., Zhao, Z., Zhang, H., Wang, J., He, X., Chen, Y., Shi, X., Ma, C., Kwok, R. T. K., Lam, J. W. Y., Sung, H. H. Y., Williams, I. D., Wong, K. S., Wang, P., & Tang, B. Z. (2019). Functionalized Acrylonitriles with Aggregation-Induced Emission: Structure Tuning by Simple Reaction-Condition Variation, Efficient Red Emission, and Two-Photon Bioimaging [Research-article]. *Journal of the American Chemical Society*, *141*(38), 15111–15120. doi: 10.1021/jacs.9b06196
28. Paquin, F., Rivnay, J., Salleo, A., Stingelin, N., & Silva, C. (2015). Multi-phase semicrystalline microstructures drive exciton dissociation in neat plastic semiconductors. *J. Mater. Chem. C*, *3*, 10715–10722. doi: 10.1039/b000000x
29. Paramasivam, M., & Kanvah, S. (2016). Rational Tuning of AIEE Active Coumarin Based α-Cyanostilbenes toward Far-Red/NIR Region Using Different π-Spacer and Acceptor Units. *The Journal of Physical Chemistry C*, *120*(20), 10757–10769. doi: 10.1021/acs.jpcc.6b01334
30. Shi, B., Jie, K., Zhou, Y., Zhou, J., Xia, D., & Huang, F. (2016). Nanoparticles with Near-Infrared Emission Enhanced by Pillararene-Based Molecular Recognition in Water. *Journal of the American Chemical Society*, *138*(1), 80–83. doi: 10.1021/jacs.5b11676
31. Su, W., Gong, T.-J., Xiao, B., & Fu, Y. (2015). Rhodium(<scp>iii</scp>)-catalyzed cyanation of vinylic C–H bonds: N-cyano-N-phenyl-p-toluenesulfonamide as a cyanation reagent. *Chemical Communications*, *51*(59), 11848–11851. doi: 10.1039/C4CC09790D
32. Suzuki, K., Kobayashi, A., Kaneko, S., Takehira, K., Yoshihara, T., Ishida, H., Shiina, Y., Oishi, S., & Tobita, S. (2009). Reevaluation of absolute luminescence quantum yields of standard solutions using a spectrometer with an integrating sphere and a back-thinned CCD detector. *Physical Chemistry Chemical Physics*, *11*(42), 9850–9860. doi: 10.1039/b912178a
33. Wang, C., & Li, Z. (2017). Molecular conformation and packing: Their critical roles in the emission performance of mechanochromic fluorescence materials. *Materials Chemistry Frontiers*, *1*(11), 2174–2194. doi: 10.1039/c7qm00201g
34. Wang, M., Zhang, G., Zhang, D., Zhu, D., & Tang, B. Z. (2010). Fluorescent bio/chemosensors based on silole and tetraphenylethene luminogens with aggregation-induced emission feature. *Journal of Materials Chemistry*, *20*(10), 1858–1867. doi: 10.1039/b921610c
35. Wang, T., & Jiao, N. (2014). Direct Approaches to Nitriles via Highly Efficient Nitrogenation Strategy through C–H or C–C Bond Cleavage. *Accounts of Chemical Research*, *47*(4), 1137–1145. doi: 10.1021/ar400259e
36. Wang, X., & Studer, A. (2018). Metal-Free Direct C−H Cyanation of Alkenes. *Angewandte Chemie International Edition*, *57*(36), 11792–11796. doi: 10.1002/anie.201807303
37. Wei, P., Zhang, J.-X., Zhao, Z., Chen, Y., He, X., Chen, M., Gong, J., Sung, H. H.-Y., Williams, I. D., Lam, J. W. Y., & Tang, B. Z. (2018). Multiple yet Controllable Photoswitching in a Single AIEgen System. *Journal of the American Chemical Society*, *140*(5), 1966–1975. doi: 10.1021/jacs.7b13364
38. Xing, P., & Zhao, Y. (2016). Multifunctional nanoparticles self-assembled from small organic building blocks for biomedicine. *Advanced Materials*, *28*(34), 7304–7339. doi: 10.1002/adma.201600906
39. Yu, C. Y. Y., Xu, H., Ji, S., Kwok, R. T. K., Lam, J. W. Y., Li, X., Krishnan, S., Ding, D., & Tang, B. Z. (2017). Mitochondrion-

Anchoring Photosensitizer with Aggregation-Induced Emission Characteristics Synergistically Boosts the Radiosensitivity of Cancer Cells to Ionizing Radiation. *Advanced Materials*, *29*(15), 1–9. doi: 10.1002/adma.201606167

40. Yu, Q., Chen, S., Han, C., Guo, H., & Yang, F. (2020). High solid fluorescence of novel tetraphenylethene-porphyrin. *Journal of Luminescence*, *220*(November 2019). doi: 10.1016/j.jlumin.2019.117017
41. Yuan, L., Lin, W., Zheng, K., He, L., & Huang, W. (2013). Far-red to near-infrared analyte-responsive fluorescent probes based on organic fluorophore platforms for fluorescence imaging. *Chemical Society Reviews*, *42*(2), 622–661. doi: 10.1039/c2cs35313j
42. Zhang, X., Zhang, X., Yang, B., Zhang, Y., & Wei, Y. (2014). A new class of red fluorescent organic nanoparticles: Noncovalent fabrication and cell imaging applications. *ACS Applied Materials and Interfaces*, *6*(5), 3600–3606. doi: 10.1021/am4058309
43. Zhao, J., Chi, Z., Zhang, Y., Mao, Z., Yang, Z., Ubba, E., & Chi, Z. (2018). Recent progress in the mechanofluorochromism of cyanoethylene derivatives with aggregation-induced emission. *Journal of Materials Chemistry C*, *6*(24), 6327–6353. doi: 10.1039/c8tc01648h
44. Zhu, L., Ang, C. Y., Li, X., Nguyen, K. T., Tan, S. Y., Ågren, H., & Zhao, Y. (2012). Luminescent Color Conversion on Cyanostilbene-Functionalized Quantum Dots via In-situ Photo-Tuning. *Advanced Materials*, *24*(29), 4020–4024. doi: 10.1002/adma.201200709

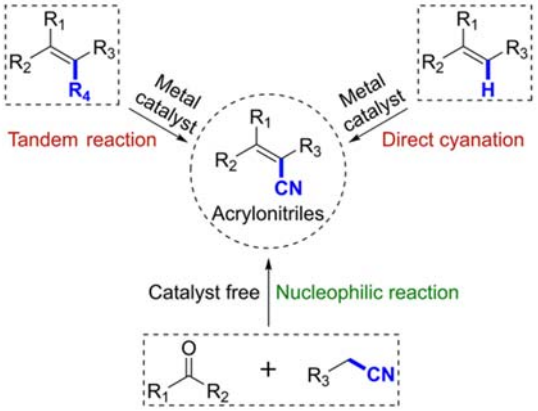

Scheme 1. *Various Strategies to Synthesize Functionalized Acrylonitriles.*

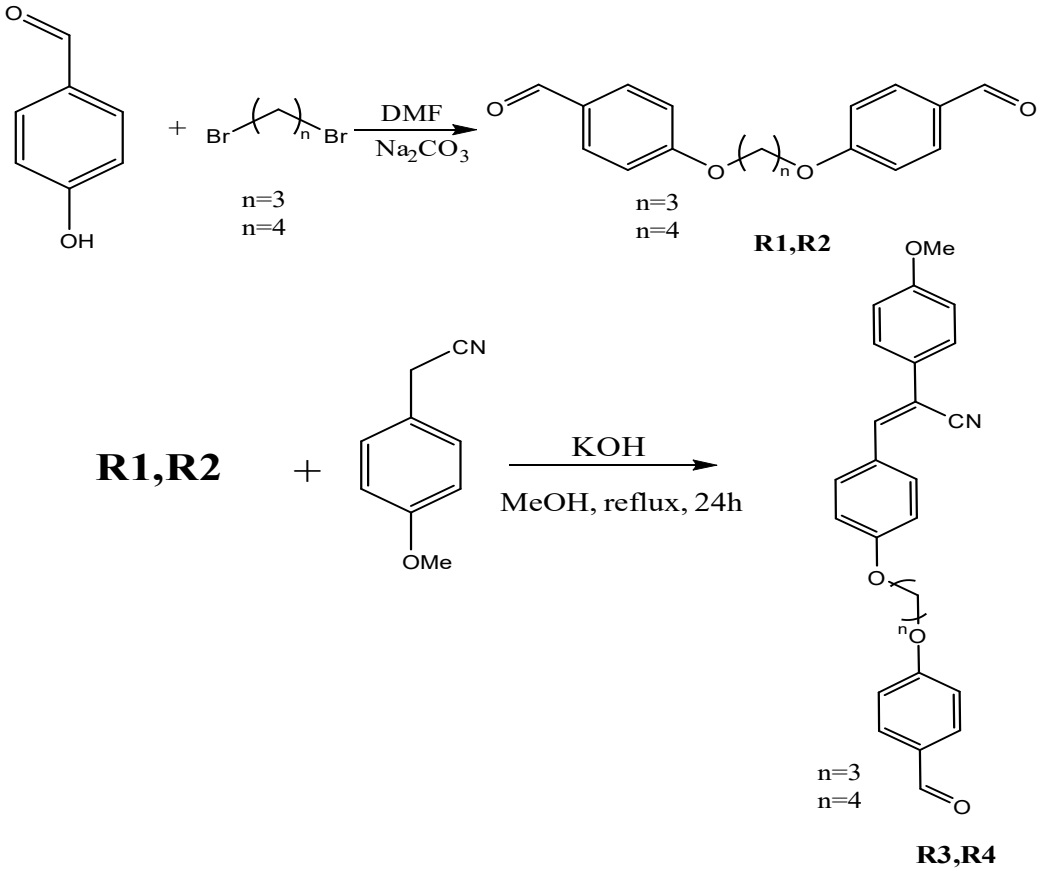

Scheme 2. *Synthesis Routes to R3, R4*

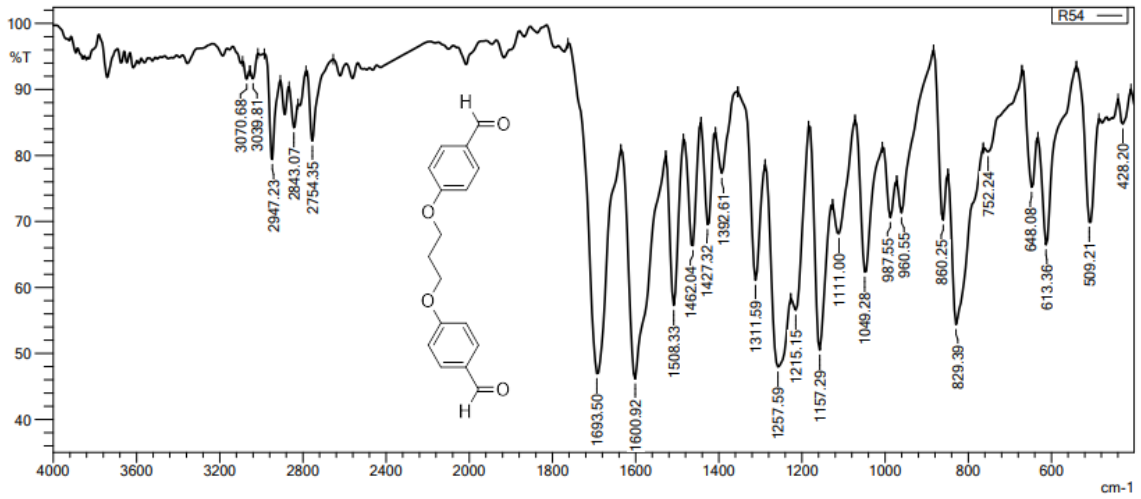

Figure 1. *IR Spectrum of the compound R1*

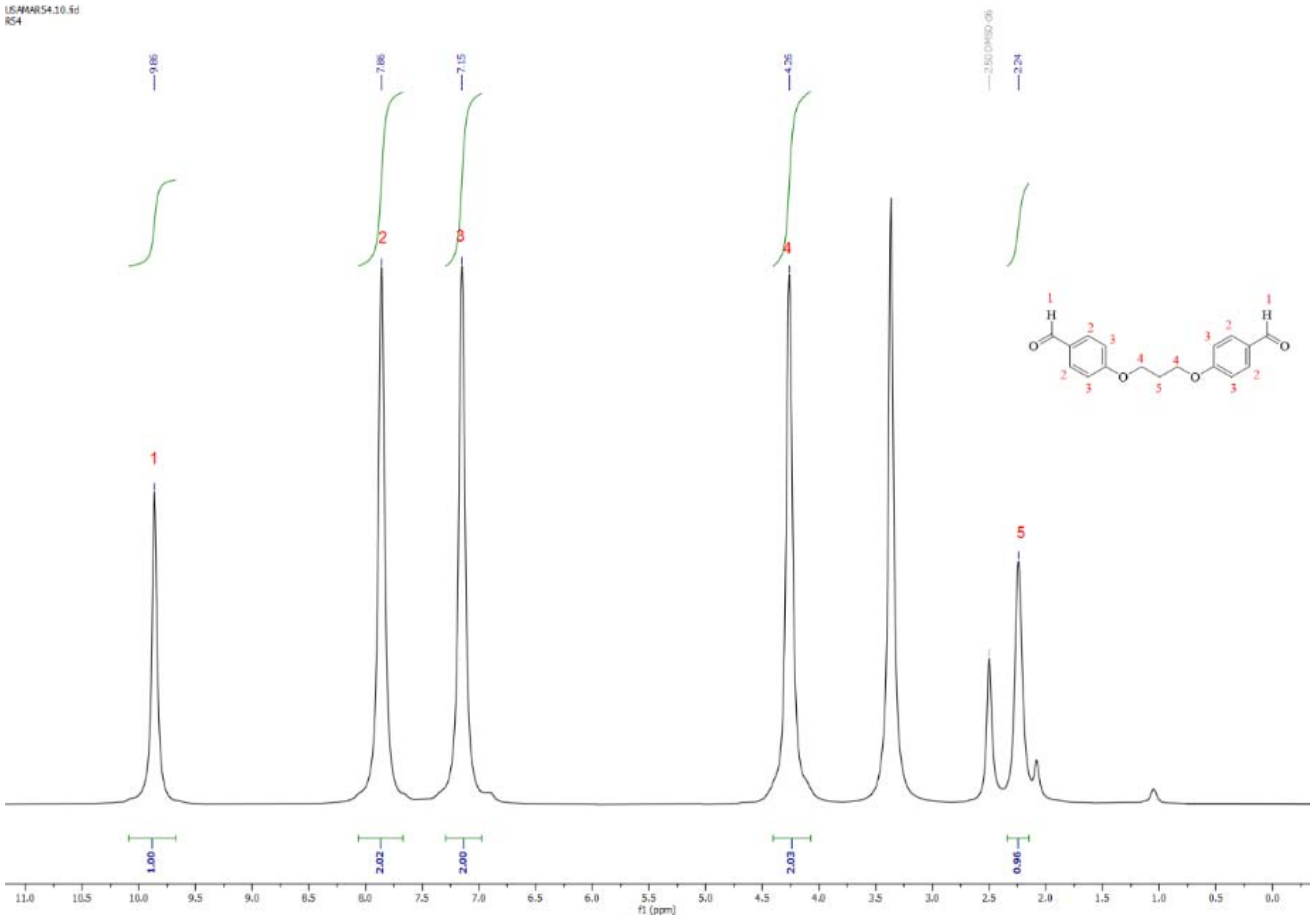

Figure 2. *[1]HNMR Spectrum of the compound R1*

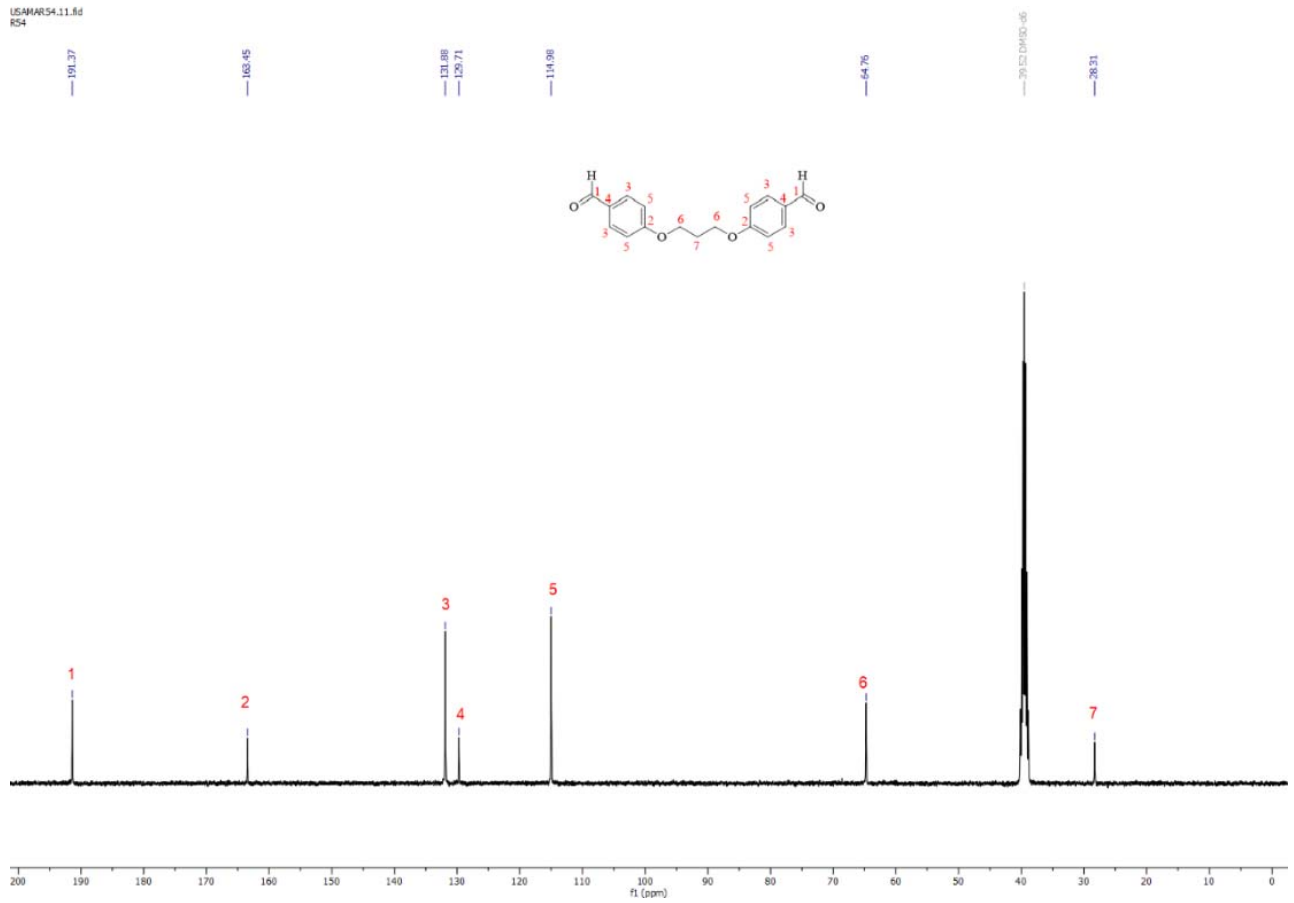

Figure 3. *^{13}CNMR Spectrum of the compound R1*

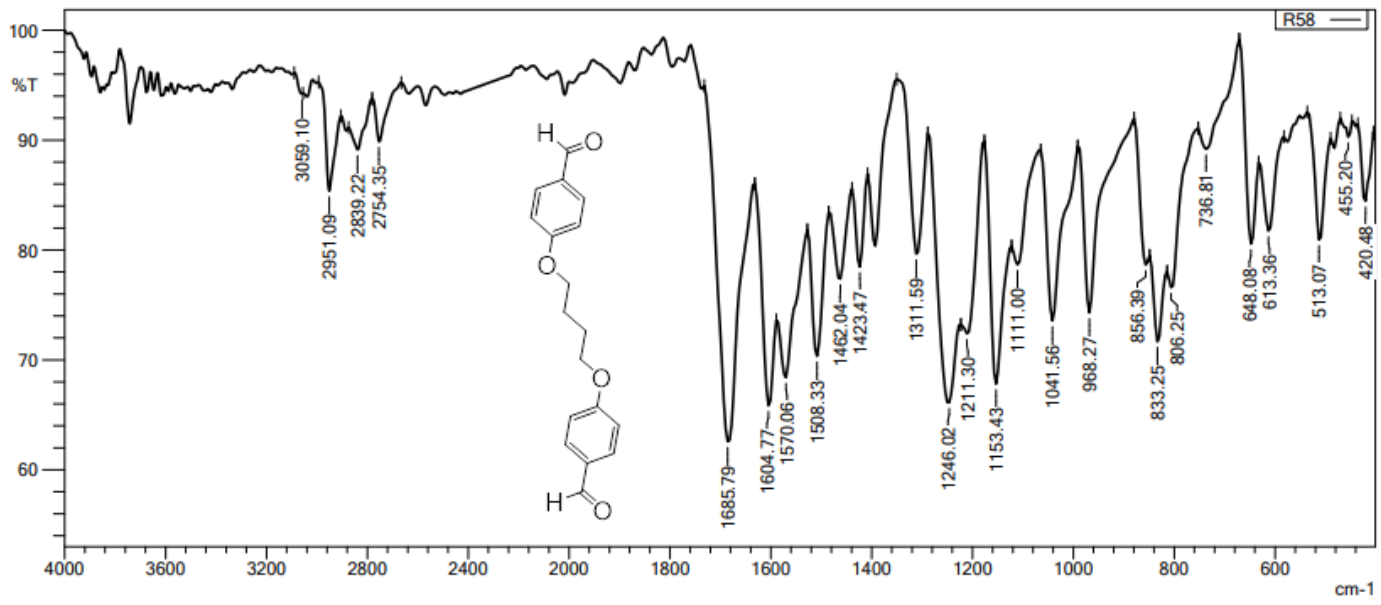

Figure 4. *IR Spectrum of the compound R2*

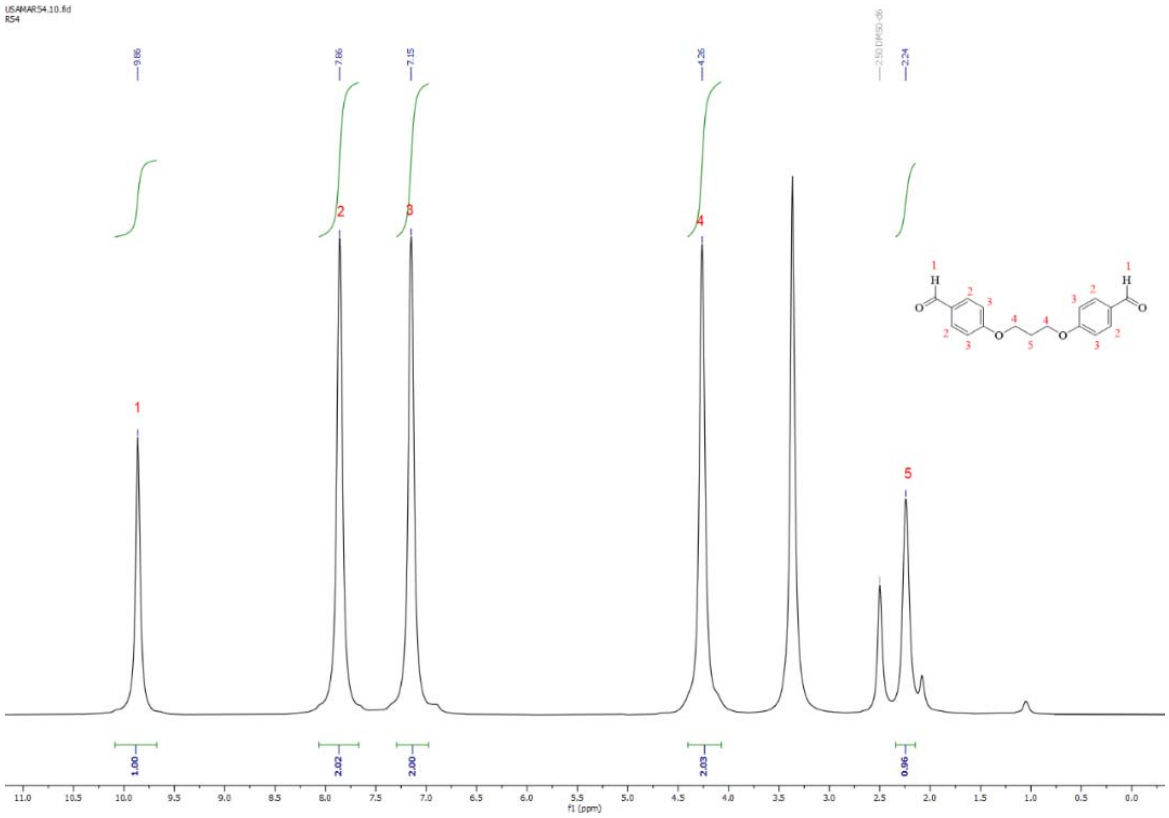

Figure 5. *[1]HNMR Spectrum of the compound R2*

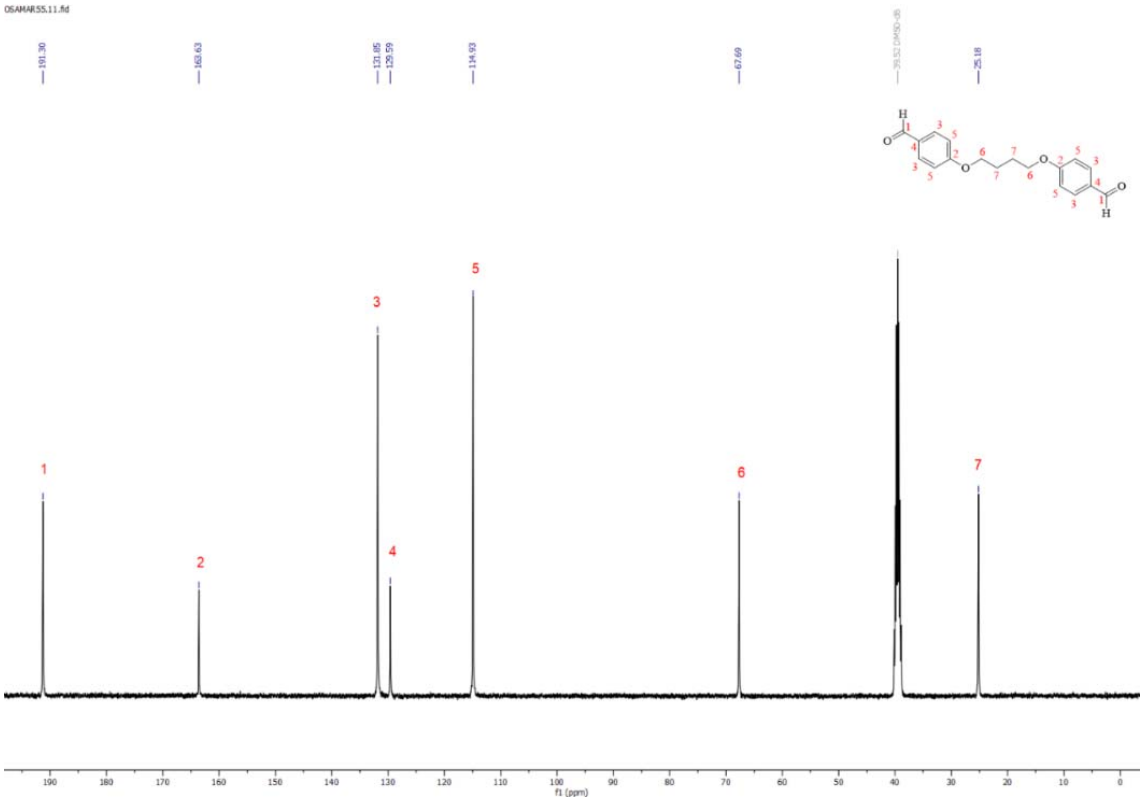

Figure 6. *[13]CNMR Spectrum of the compound R2*

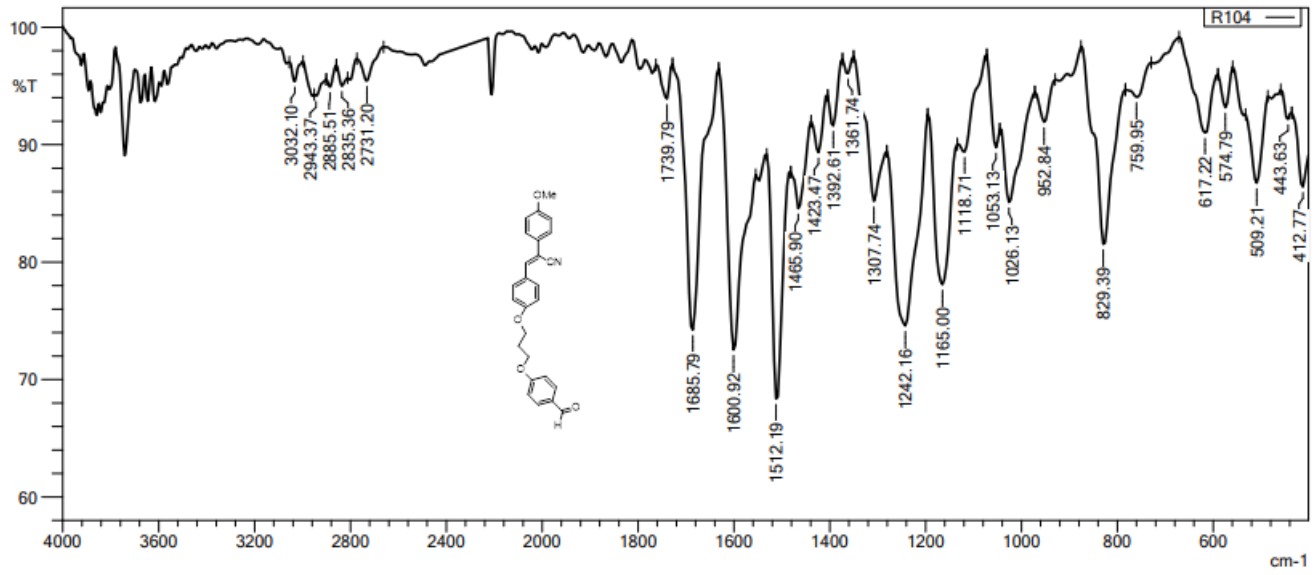

Figure 7. *IR Spectrum of the compound R3*

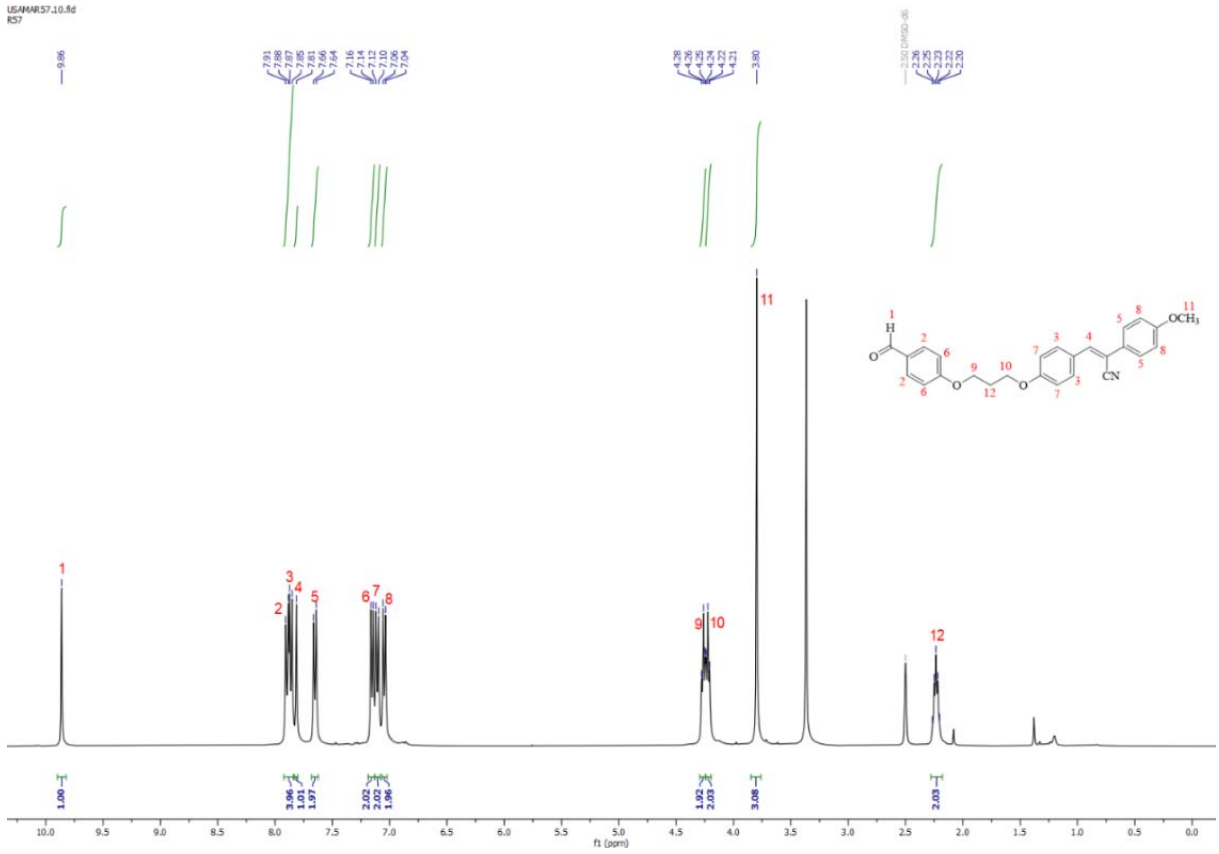

Figure 8. *[1]HNMR Spectrum of the compound R3*

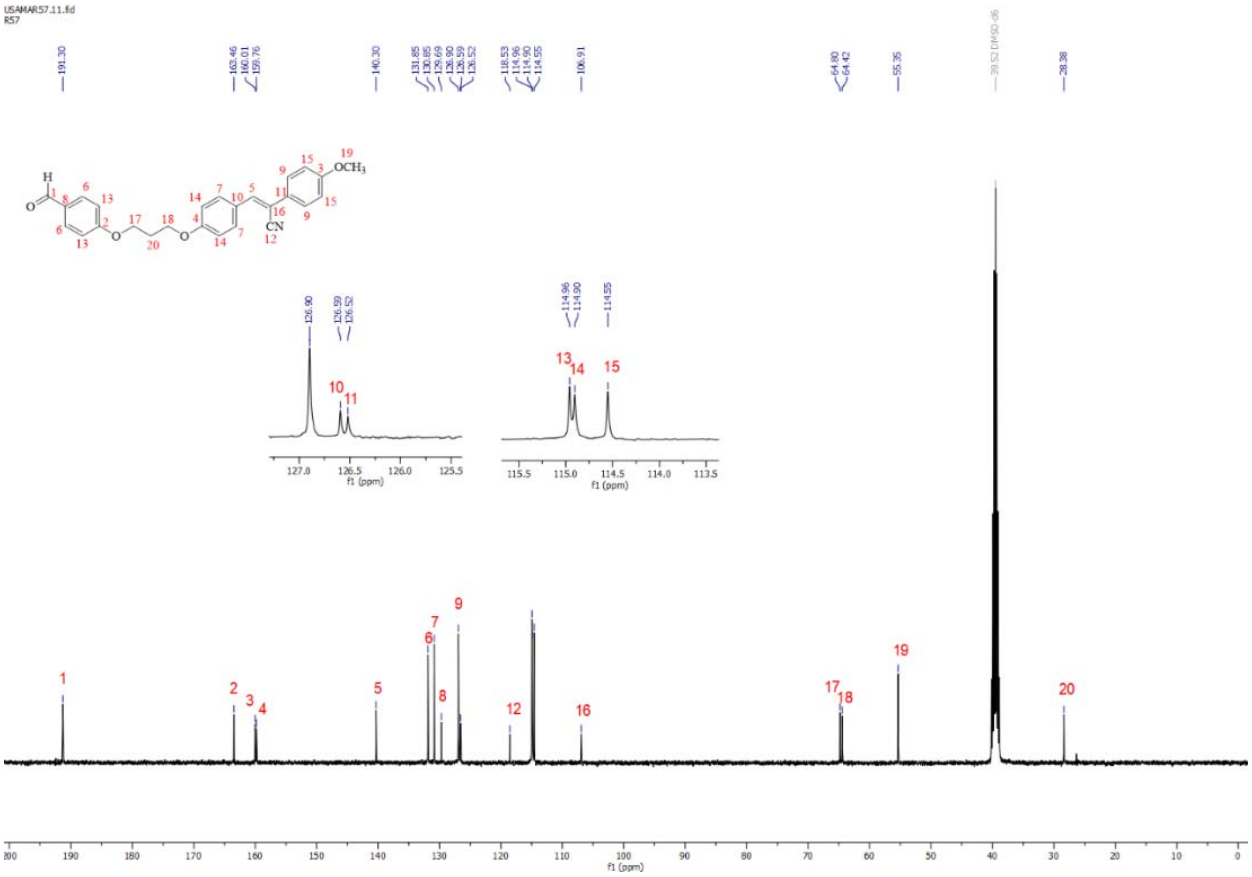

Figure 9. *^{13}CNMR Spectrum of the compound R3*

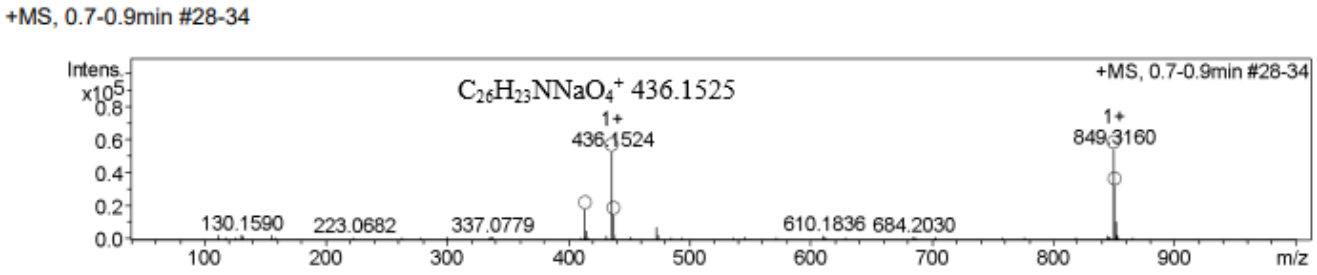

Figure 10. *Mass Spectrum (ESI) of the compound R3*

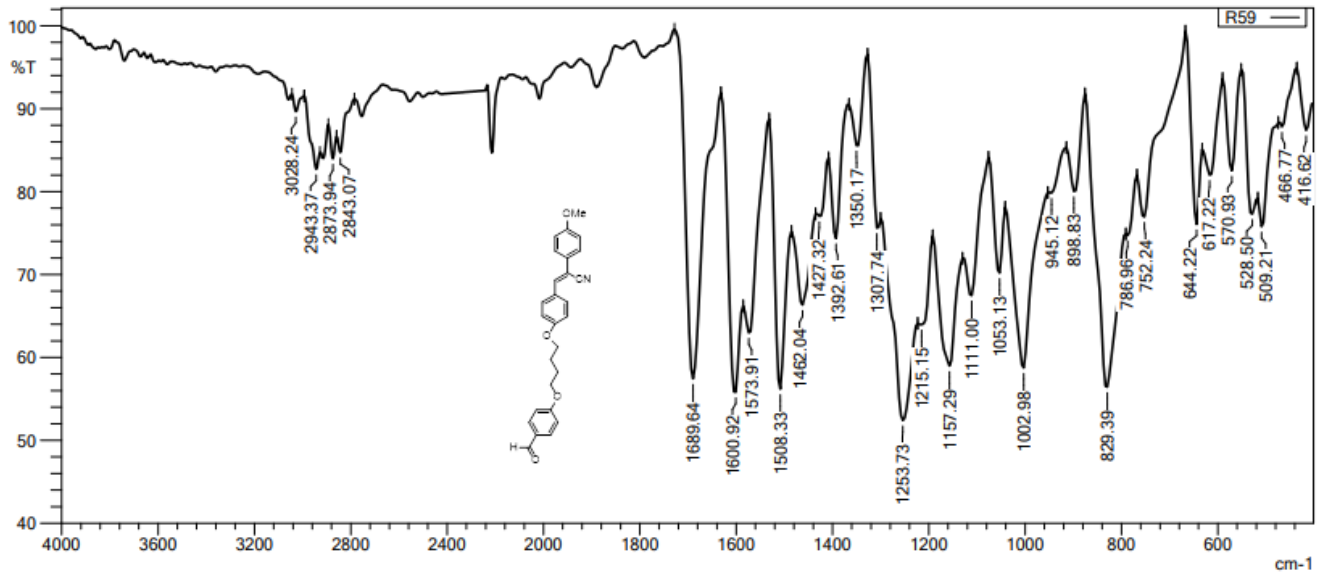

Figure 11. *IR Spectrum of the compound R4*

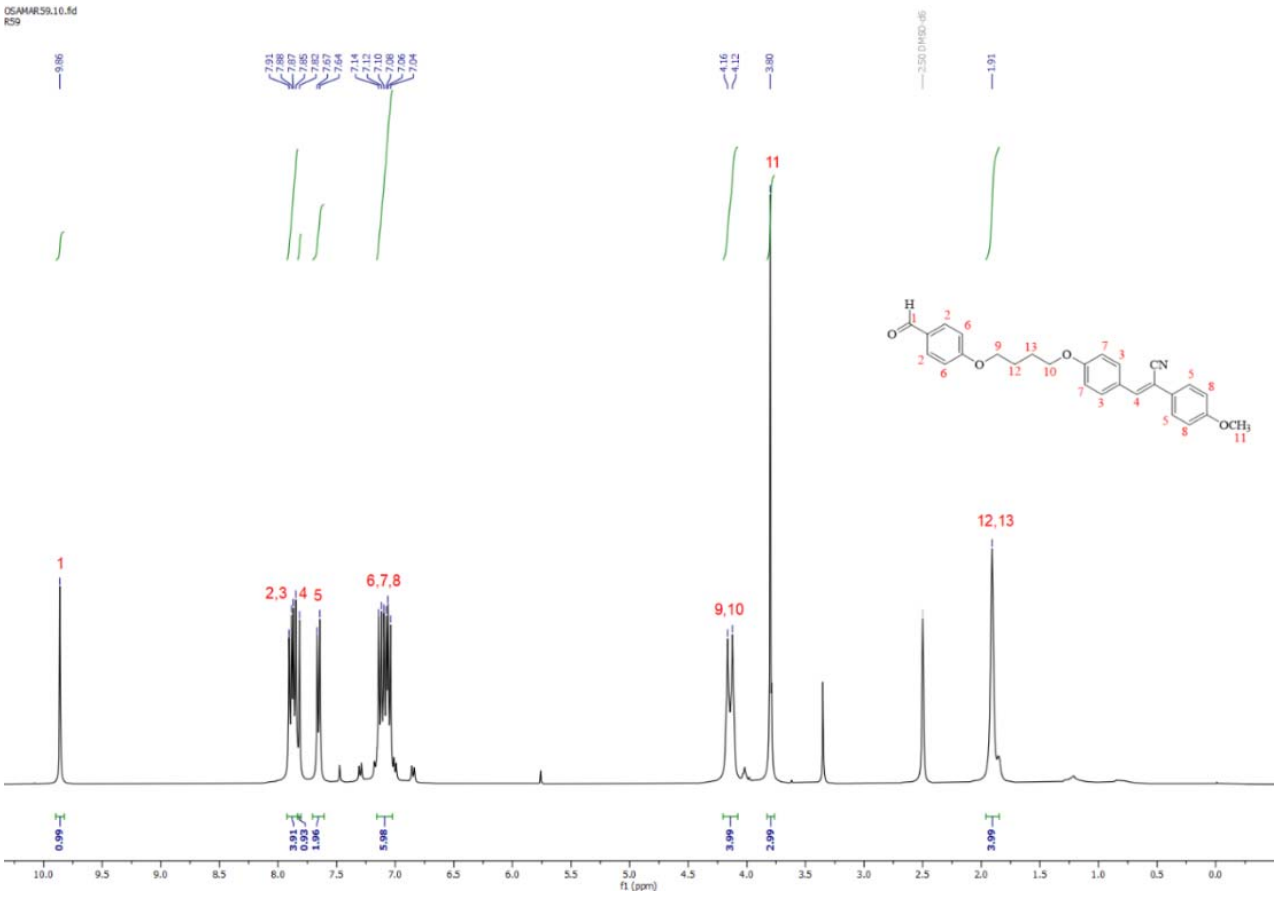

Figure 12. *[1]HNMR Spectrum of the compound R4*

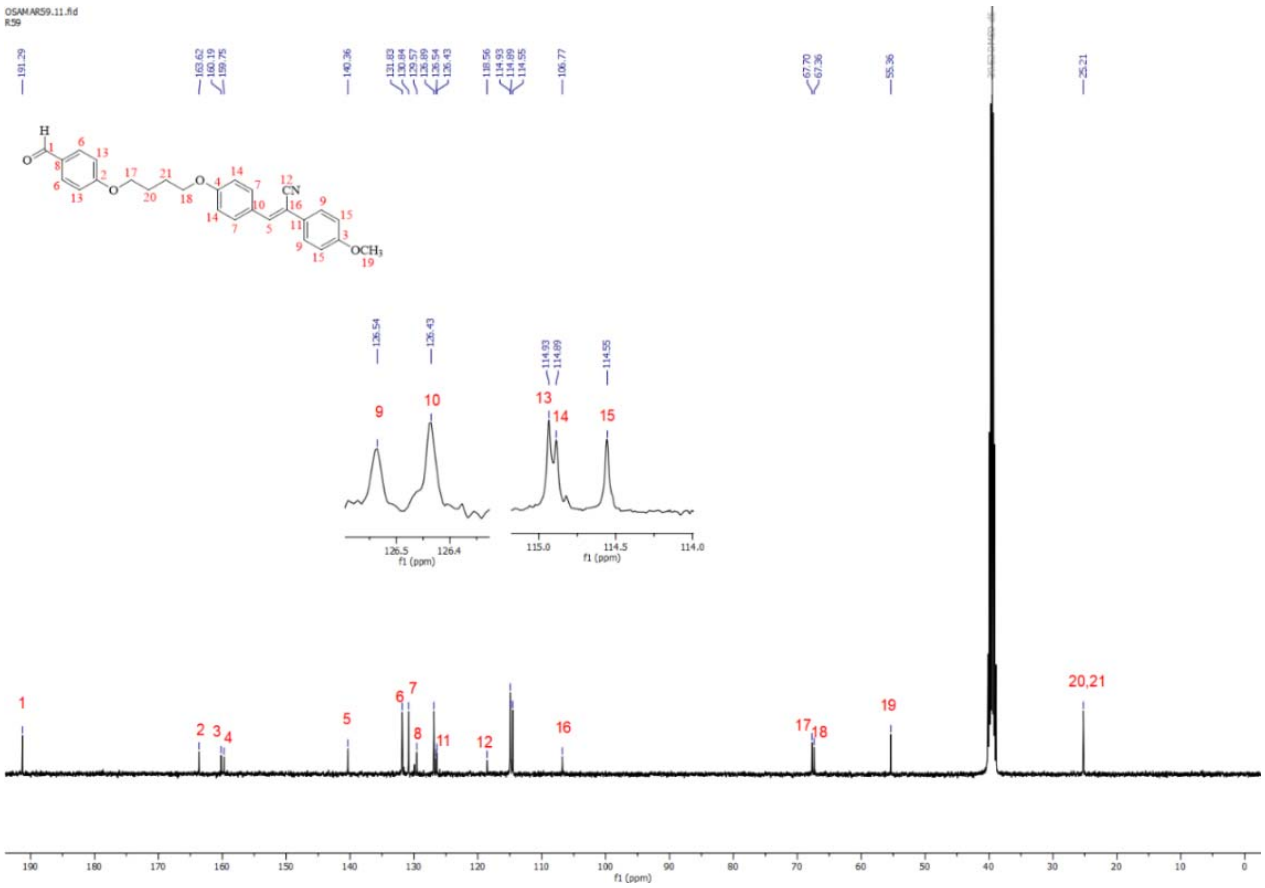

Figure 13. *^{13}CNMR Spectrum of the compound R4*

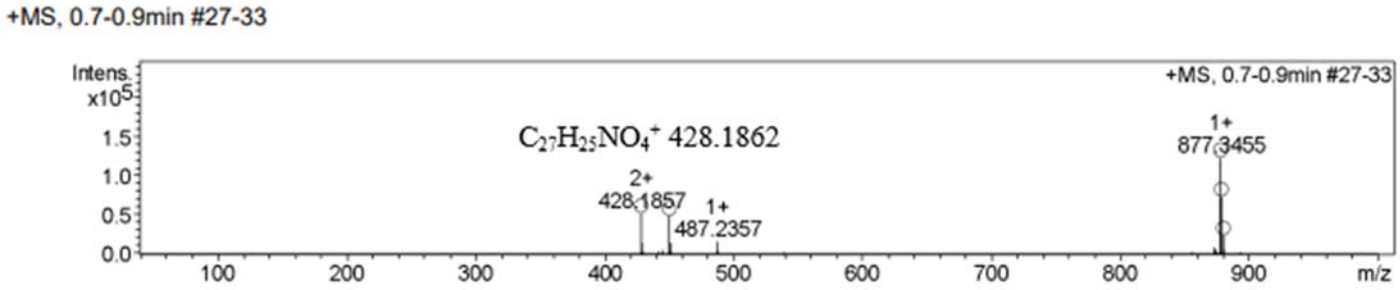

Figure 14. *Mass Spectrum (ESI) of the compound R4*

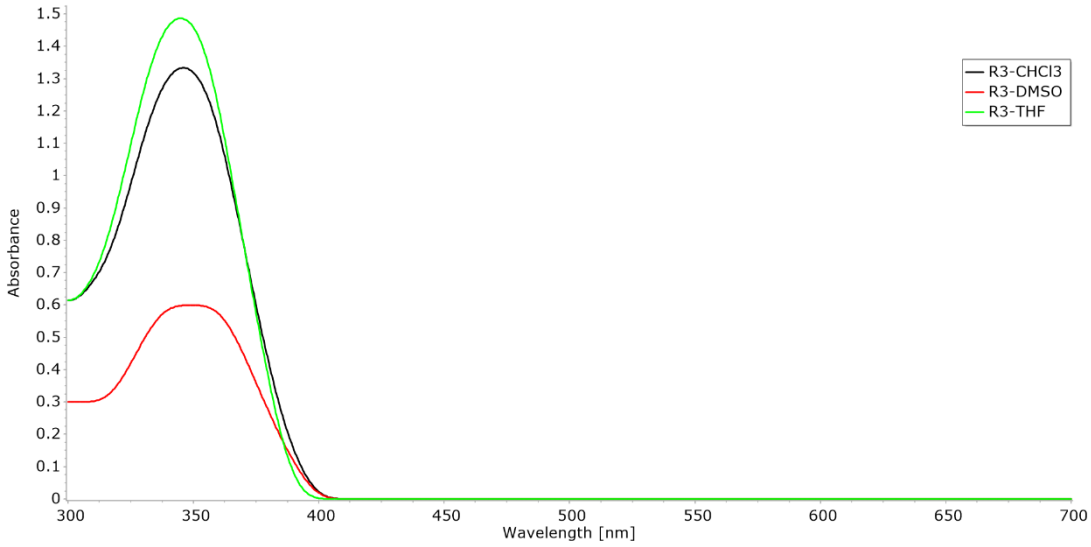

Figure 15. *The absorption spectra of compound R3 in different solvents (1×10^{-5} M)*

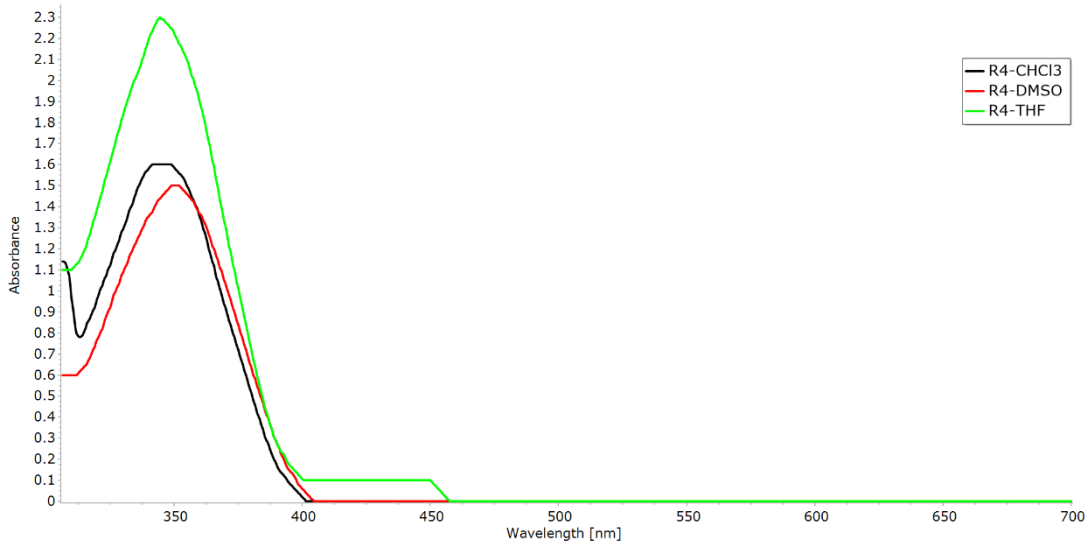

Figure 16. *The absorption spectra of compound R4 in different solvents (1×10^{-5} M)*

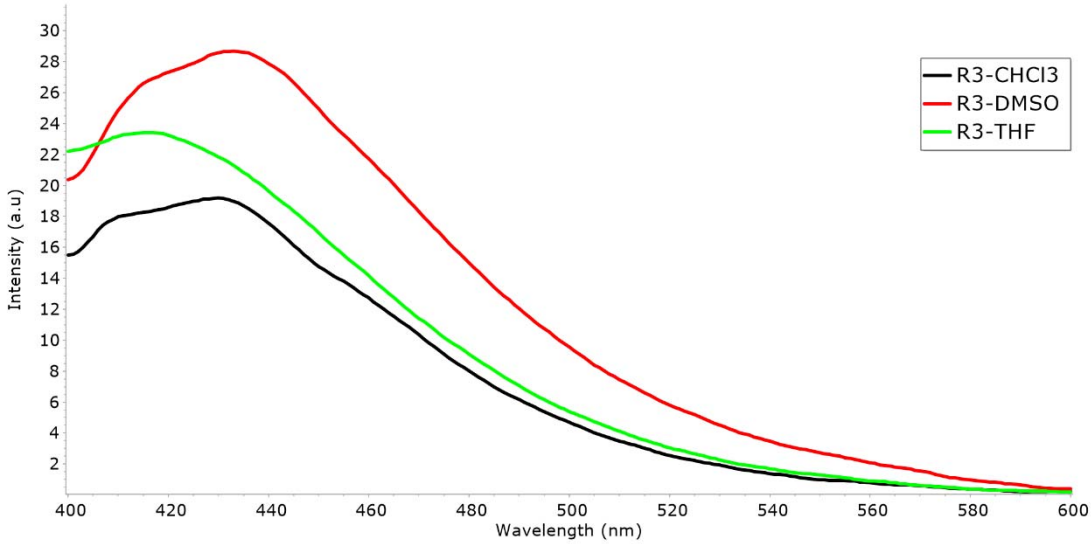

Figure 17. *The emission spectra of compound R3 in different solvents (1×10^{-5} M) excited at λ= 350 nm.*

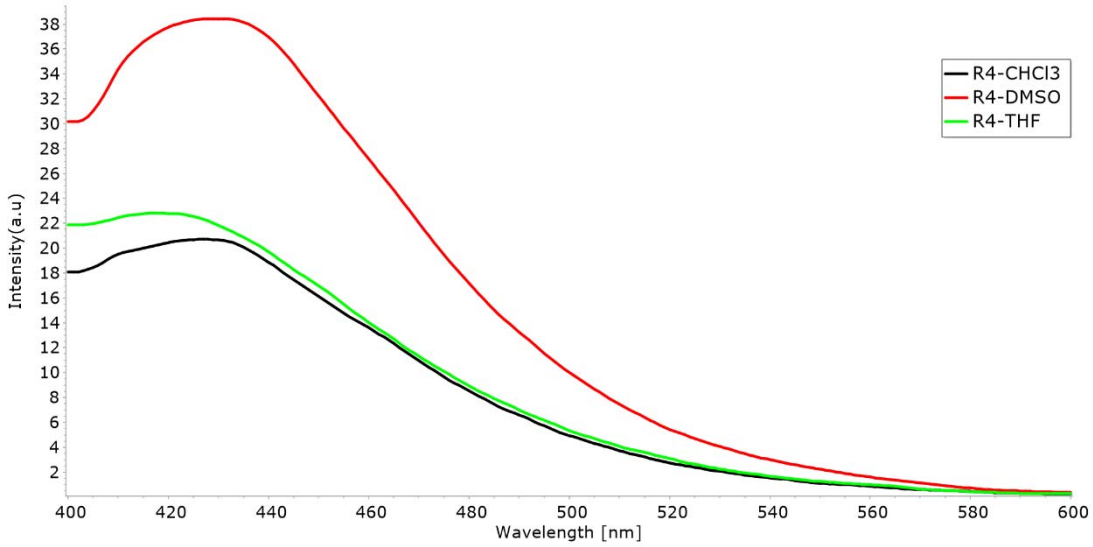

Figure 18. *The emission spectra of compound R4 in different solvents (1×10^{-5} M) excited at λ= 350 nm.*

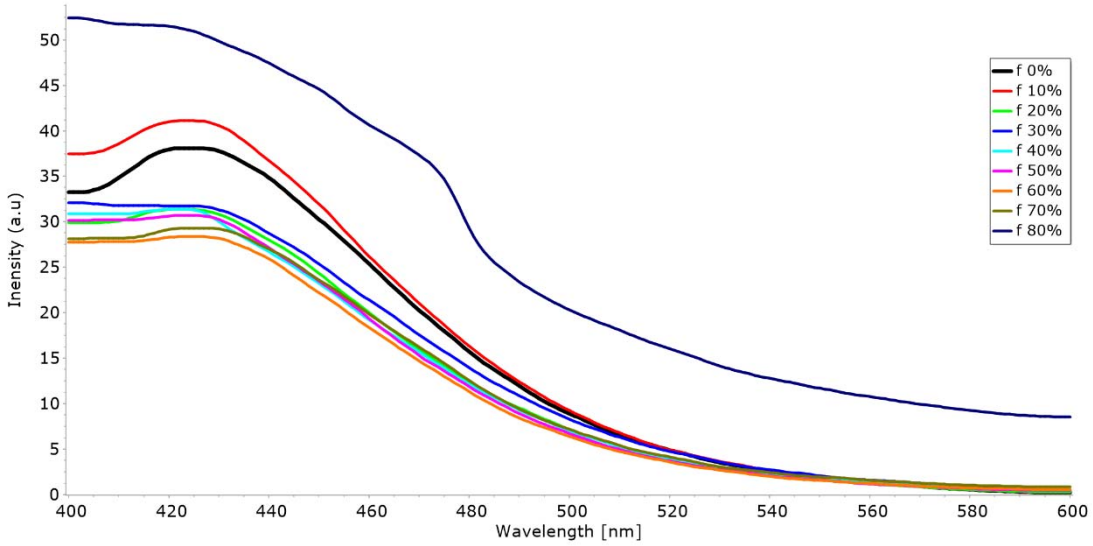

Figure 19. *The emission spectra of compound R3 with different fractions of H_2O in THF/H_2O mixtures (1μM) excited at λ = 350 nm.*

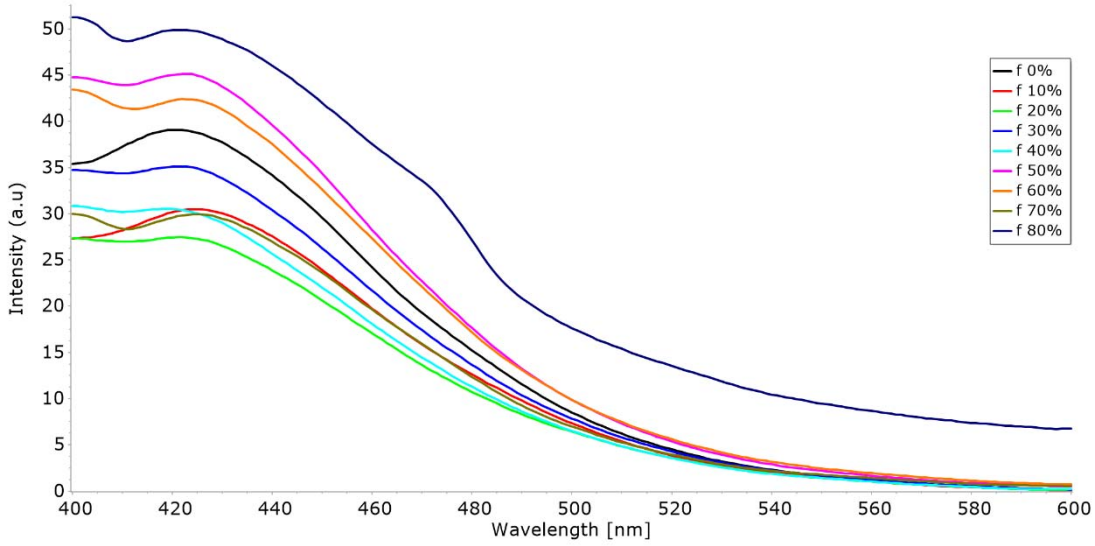

Figure 20. *The emission spectra of compound R4 with different fractions of H_2O in THF/H_2O mixtures (1μM) excited at λ = 350 nm.*

Table 1. Absorption and fluorescence data of samples R3 and R4 in solvents at 298 K.

Samples.	**λ_{abs}/nm**	**ε**(L mol^{-1} cm^{-1})	**λ_{em}/nm**	**Stokes shift/nm**	**Φ_f**	**Solvent**
Tryptophan	278.5	230000	280	-	0.15	Water
R3	345	150000	417	72	0.021	
R4	342	230000	416	74	0.014	THF
R3	345	140000	431	86	0.021	
R4	346	160000	425	79	0.02	$CHCl_3$
R3	350	70000	434	84	0.071	
R4	350	150000	432	82	0.035	DMSO